TISSUE ENGINEERING: Part A
Volume 19, Numbers 23 and 24, 2013

DOI: 10.1089/ten.tea.2013.0075

Hybrid Hydroxyapatite Nanoparticle Colloidal Gels are Injectable Fillers for Bone Tissue Engineering

Qun Wang, PhD,[1,2] Zhen Gu, PhD,[3] Syed Jamal, MS,[4]
Michael S. Detamore, PhD,[4] and Cory Berkland, PhD[4,5]

Injectable bone fillers have emerged as an alternative to the invasive surgery often required to treat bone defects. Current bone fillers may benefit from improvements in dynamic properties such as shear thinning during injection and recovery of material stiffness after placement. Negatively charged inorganic hydroxyapatite (HAp) nanoparticles (NPs) were assembled with positively charged organic poly(D,L-lactic-co-glycolic acid) (PLGA) NPs to create a cohesive colloidal gel. This material is held together by electrostatic forces that may be disrupted by shear to facilitate extrusion, molding, or injection. Scanning electron micrographs of the dried colloidal gels showed a well-organized, three-dimensional porous structure. Rheology tests revealed that certain colloidal gels could recover after being sheared. Human umbilical cord mesenchymal stem cells were also highly viable when seeded on the colloidal gels. HAp/PLGA NP colloidal gels offer an attractive scheme for injectable filling and regeneration of bone tissue.

Introduction

In the United States, bone injury occurs to seven million people every year and treatments cost upward of $215 billion annually.[1,2] Repair of skeletal defects resulting from traumatic insult, tumor ablation, or congenital deformities remains a formidable challenge for surgeons.[3] Clinically, injectable fillers are attractive alternatives to surgical operations since it can reduce scar formation, infection, patient discomfort, and treatment cost.[4] Particularly, injectable scaffolds injected at low viscosity may be ideal tissue engineering scaffolds for bone repair or for delivery of cells to injured sites. This approach is minimally invasive and is capable of filling complex three-dimensional (3D) defects. The desirable injectable tissue fillers should have modest viscosity upon application and solidify or transition to high viscosity upon settlement. Normally, injectable tissue fillers are chemically crosslinked to polymerize the material. Unfortunately, toxic chemicals are often applied in this process. These agents may negatively affect the scaffolds, destabilize loaded biomolecules, and pose toxicity concerns.

Colloidal gels with 3D microporous structures composed of nanomaterials were manufactured to overcome these drawbacks.[5–7] These systems comprised oppositely charged nanoparticles (NPs) with high solid contents solidifying the material through interparticle interactions.[8,9] Owing to short range and temporary electrostatic forces and van der Waals attraction, colloidal gels with unique pseudoplastic behavior facilitated the formation of shape-specific injectable tissue fillers with porous microstructures.[10,11] Recent research has leveraged similar advantages to achieve special bulk materials for various applications,[12–17] including colloidal gels aimed toward regenerating tissues.[18,19] The unique properties of high-concentration, cohesive colloidal gels make it a potential candidate as an injectable filler to repair bone, such as craniofacial defects.

Hydroxyapatite (HAp) NPs represent an attractive building block for colloidal gels. HAp is a native mineral component of bone that has already been approved by the Food and Drug Administration for craniofacial repairs.[3,20–22] This osteogenic and bioresorbable material can interact with neighboring bone and can be replaced by new bone.[23,24] Moreover, HAp has been found to be an effective substrate for cell attachment and expression of osteoblast phenotypes.[25,26]

Colloidal gels must also be compatible with native tissue and/or with progenitor cells that can further stimulate regeneration of tissue. Human mesenchymal stem cells can differentiate into adipocytes, chondrocytes, neurons, fibroblasts, myoblasts, and osteoblasts.[27–31] Compared to human bone marrow mesenchymal stem cells, human umbilical cord mesenchymal stem cells (hUCMSCs) may be advantageous because of ready availability, noninvasive acquisition, and minimal ethical issues. hUCMSCs also exhibit desirable plasticity and developmental flexibility.[27] Furthermore, hUCMSCs appear to minimize or eliminate rejection by the immune system as compared to other cell sources.[27]

[1]Department of Chemical and Biological Engineering and [2]Department of Civil, Construction and Environmental Engineering, Iowa State University, Ames, Iowa.
[3]Joint Department of Biomedical Engineering, University of North Carolina at Chapel Hill and North Carolina State University, Raleigh, North Carolina.
[4]Department of Chemical and Petroleum Engineering and [5]Department of Pharmaceutical Chemistry, University of Kansas, Lawrence, Kansas.

The aim of this work was to create colloidal gels from natural materials and to evaluate compatibility with hUCMSCs. Here, negatively charged HAp NPs were combined with positively charged poly(D,L-lactic-co-glycolic acid) (PLGA) NPs to form an injectable colloidal gel bone tissue filler. PLGA NPs were surface-modified chitosan, a naturally occurring polysaccharide that has been widely used in tissue scaffolds.[32–35] Injectable bone fillers were created by mixing the negatively charged HAp NPs and positively charged PLGA NPs in ratios. At certain compositions, colloidal gels exhibited a yield point indicative of Bingham plastic behavior, but were also shear thinning. The negligible cytotoxicity to hUCMSCs and desirable rheological behavior supported potential translation of these materials for bone tissue engineering.

Materials and Methods

Materials

All materials were purchased from Fisher Scientific, Inc. unless otherwise stated. PLGA (75:25) (7525 DLG 2.5E) was obtained from Lakeshore Biomaterials. Chitosan with a degree of deacetylation at 75%–85% and Mn at 612 kDa were purchased from Sigma-Aldrich Co.

Preparation of negatively charged HAp NPs

Negatively charged HAp NPs were prepared by precipitation of calcium chloride and sodium phosphate in an alkaline medium, according to the reaction:

$$5CaCl_2 \cdot 2H_2O + 3Na_2HPO_4 \cdot 7H_2O + 4OH^- = Ca_5(PO_4)_3(OH) + 6NaCl + 34H_2O + 4Cl^-$$

A ten milliliter $CaCl_2 \cdot 2H_2O$ solution with a concentration 0.1 M was added into a 100 mL $Na_2HPO_4 \cdot 7H_2O$ solution with a concentration 0.006 M through a pump at 30 mL/h under stirring at 200 rpm. The pH of the suspension was adjusted to 10 by adding the NaOH solution with a concentration 2 M. Poly (acrylic acid) (PAA) was used as a crystal growth inhibitor at a constant concentration 50 ppm. NPs were washed and collected by a high-speed centrifuge (Avanti 30; Beckman Co.) (14,000 rpm, 15 min). A fine powder of NPs available for usage was obtained by lyophilization.

Preparation of positively charged PLGA NPs

Positively charged PLGA NPs were fabricated through a solvent diffusion method. One hundred milligrams of PLGA was dissolved in 10 mL of acetone followed by addition into a 0.2% chitosan solution. Stirring remained overnight to evaporate excess acetone. NPs were washed and collected by high-speed centrifuge to remove excess chitosan. A fine powder of NPs available for usage was obtained by lyophilization.

Preparation of colloidal gels

Lyophilized NPs (HAp or PLGA) were dispersed in deionized water at the reported concentrations and ratios. Homogeneous mixtures were obtained in a bath sonicator for 3 min and stored at 4°C for 2 h allowing structural organization before use. Colloidal gels with different ratios of HAp NPs and PLGA NPs were designated as H100, HP73, HP55, HP37, and P100 (H: HAp NPs; P: PLGA NPs; the weight ratios of HAp NPs to PLGA NPs were 100:0, 70:30, 50:50, 30:70, and 0:100, respectively).

Characterization of NPs and colloidal gels

Sizes and zeta potentials of the HAp and PLGA NPs were measured by the ZetaPALS dynamic light scattering instrument (ZetaPALS; Brookhaven). All samples were tested in triplicate. The Fourier Transform Infrared Spectroscopy (FTIR) spectra of different NPs and colloidal gels were obtained using an FTIR spectrometer (Prota Type; ABB Bomem) after mixing with KBr pellets. The X-ray diffraction patterns of different NPs and colloidal gels were determined using a Shimadzu Lab-XRD-6000× diffractometer, with nickel-filtered CuKα radiation at 40 kV and 50 mA in the 2θ range of 5° – 45°.

Scanning electron microscopy (SEM) was performed by the Jeol JSM-6380 field emission scanning electron microscope at the accelerating voltage of 10 kV. Briefly, the colloidal gels were suspended in distilled water and subsequently evaporated in droplets onto the carbon tape of the SEM stub. Thereafter, gold coating was performed and samples were stored for future use. Atomic force microscopy (AFM) images were obtained at ambient conditions using a Multimode Nanoscope E Atomic Force Microscope (Veeco Instruments) operating in a contact mode. Samples were prepared via evaporation of colloidal gel suspension on a glass cover slip at room temperature followed by spin coating. Dry samples were scanned by Veeco silicon nitride tips with a force constant of 0.12 N/m at 2 Hz with a set point of ~1–2 V for all images.

Rheological experiments

Rheological experiments were performed on the controlled stress rheometer (AR2000; TA Instrument, Ltd.). A 2° cone steel plate (20 mm diameter) was used and the 500-μm gap was filled with a colloidal gel. A solvent trap filled with distilled water was used to prevent evaporation of water. The viscosity (η) was monitored and the recoverability was assessed at specific time breaks between cycles. All experiments were performed in triplicate.

Cytotoxicity

hUCMSCs were isolated and cultured as previously described.[36] Before cell seeding, the colloidal gels were sterilized under UV light for 20 min. Cells were deposited on colloidal gels in each well of 12-well polystyrene culture plates with cell density of 1×10^4 cells/well. Then, 2 mL of culture medium was added into wells. Cells were cultured in a monolayer onto the gel surface for 2 weeks, with half of the media changed every other day. Cells cultured in blank polystyrene tissue culture plates were used as control. Subsequently, LIVE/DEAD assay was performed on the cells before being subjected to fluorescence microscopy (Nikon TS100).

Results and Discussion

Characterizations of NPs and hybrid colloidal gels

Figure 1 illustrated the fabrication of hybrid HAp/PLGA NP colloidal gels. In details, negatively charged HAp NPs were prepared by precipitation of calcium chloride and sodium phosphate in an alkaline medium. The formation of

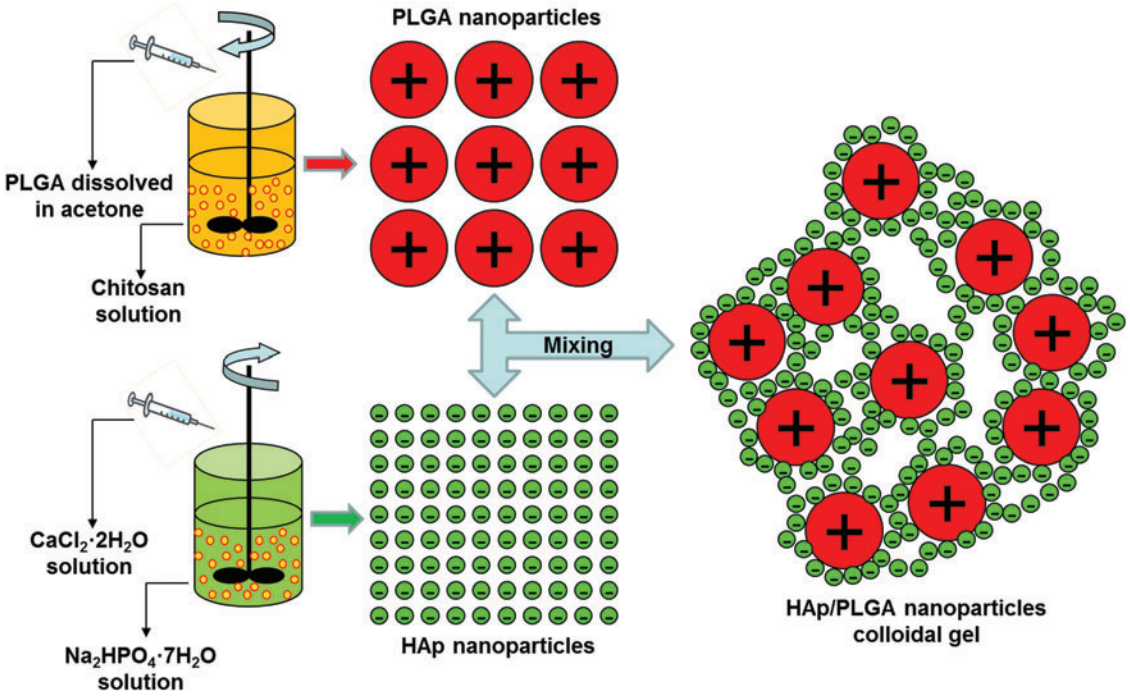

FIG. 1. Schematic representation of the process for fabrication of oppositely charged HAp and PLGA NPs and formation of the colloidal gel. HAp, hydroxyapatite; PLGA, poly(D,L-lactic-co-glycolic acid). Color images available online at www.liebertpub.com/tea

positive charged PLGA NPs occurred in the chitosan polyelectrolyte solution, resulting in a surface coating of positively charged polymers. The properties of each particle type are shown in Table 1. Zeta potential and particle size are two critical factors influencing the cohesive properties of colloidal gel systems.[15] The particle size of PLGA NPs was 10 times as that of HAp NPs and the absolute value of the particle zeta potential of PLGA NPs was much larger compared with HAp NPs. These differences influenced gel properties and made it possible to employ PLGA NPs to improve the injectability of HAp bioceramic scaffolds.

As mentioned before, colloidal gels comprised oppositely charged NPs may stiffen through physical interparticle interactions. This phenomenon can facilitate the fabrication of shape-specific materials with 3D porous structures and avoid chemical crosslinking agents normally required during solidification. Figure 2 showed the FTIR spectra and X-ray diffraction patterns of pure HAp NPs, pure PLGA NPs, and hybrid colloidal gel HP55, respectively. In Figure 2A, there were no new characteristic absorption bands in the blended colloidal gel. Figure 2B also showed no new peaks in the blended colloidal gel HP55. All the results gave strong evidence that the hybrid colloidal gels were simply a physically crosslinked system without chemical intermolecular interactions. Interestingly, due to the amorphous structure of PLGA, the absorbance in the X-ray diffraction pattern was much lower compared with HAp. And the peaks of PLGA were eventually smoothed and further disappeared in the X-ray pattern of hybrid materials.

Table 1. PLGA and HAp NP Properties

	PLGA	*HAp*
Size (nm)	218 ± 24	20 ± 1
Polydispersity	0.132	0.072
Zeta potential (mV)	+21.1 ± 1.8	−12.2 ± 1.0

HAp, hydroxyapatite. PLGA, poly(D,L-lactic-co-glycolic acid); NPs, nanoparticles.

Morphology and shape retention of hybrid colloidal gels

Oppositely charged NPs were first suspended separately in deionized water at 20% (w/w). The very small size of HAp NPs yielded a densely packed material when dried as compared to PLGA NPs (Fig. 3A, B). Mixing these two oppositely charged NPs yielded colloidal gels with differences in the internal structures as observed by SEM and AFM (Fig. 3). As the relative amount of PLGA NPs increased (Fig. 3C: HP73; 3D: HP55; 3E: HP37), colloidal gels exhibited a more open porous structure. The oppositely charged NPs assembled into small micrometer-scale agglomerates, which connected at larger scales to organize the porous bulk material. AFM micrographs of the HP55 colloidal gel (Fig. 3F) also exhibited the porous bulk structure typical of colloidal gels.

Colloidal systems comprised oppositely charged NPs exhibiting special pseudoplastic behaviors facilitating the formation of materials with a desired shape. Here, the pseudoplastic property of the colloidal system has been leveraged to construct injectable scaffolds for bone tissue engineering (Fig. 4). Figure 4A–C shows exemplary molded scaffolds of colloidal gels HP37, HP55, and HP73, respectively. The results demonstrated that gels with different compositions showed different moldability resulting from the changing ratios of oppositely charged NPs. Different colloidal gels (Fig. 4D-A indicated as HP37; D-B indicated as HP55; and D-C indicated as HP73) were put into 50-mL Falcon tubes to study

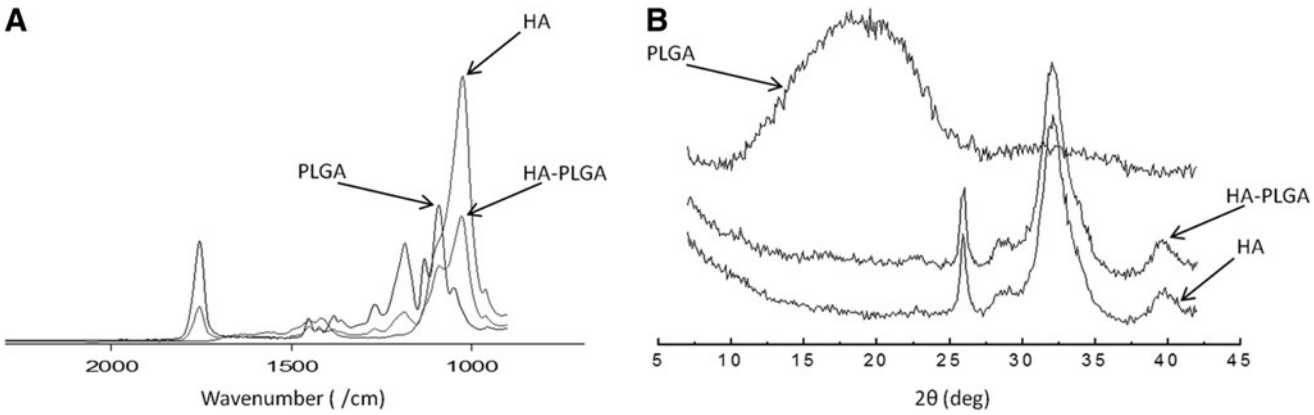

FIG. 2. Fourier Transform Infrared Spectroscopy spectra **(A)** and X-ray **(B)** diffraction patterns of pure HAp NPs (HA), pure PLGA NPs (PLGA), and hybrid HP55 colloidal gel (HA-PLGA).

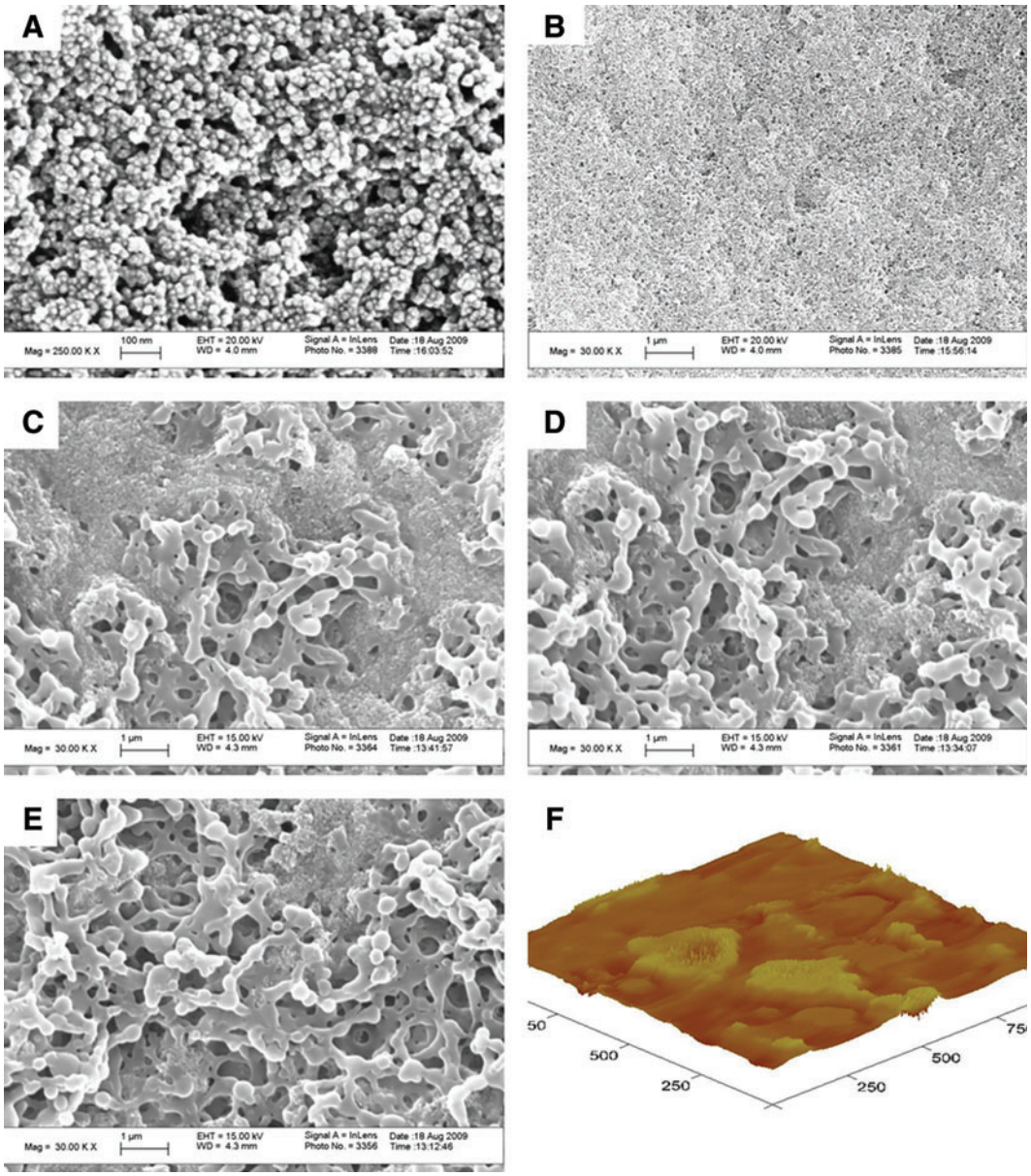

FIG. 3. Scanning electron microscopy pictures of pure HAp NPs **(A, B)**, and colloidal gels HP37 **(C)**, HP55 **(D),** and HP73 **(E)**. An atomic force microscopy picture of the colloidal gel HP55 **(F)** [scale bars were 100 nm for **(A)** and 1 μm for **(B–E)**. The unit of **(F)** was nm]. Color images available online at www.liebertpub.com/tea

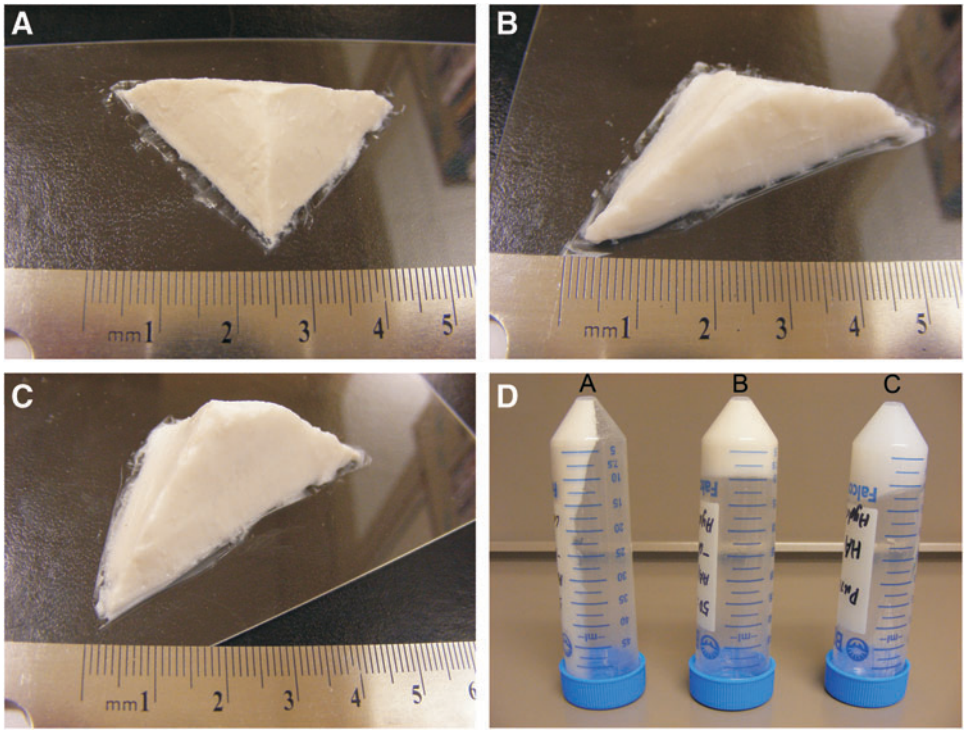

FIG. 4. Shaped tissue scaffolds made by colloidal gels HP37 **(A)**, HP55 **(B)**, HP73 **(C)**, and shape stability tests **(D [A, B, C])**. Color images available online at www.liebertpub.com/tea

shape retention. Systems composed of an overall equal charge balance (HP55 with 1:1 mass ratio, Fig. 4D-B) demonstrated less fluidity and retained their structure. This confirmed the key roll of the overall charge ratio to the structures and cohesive properties of the colloidal gels.

Shear thinning and recoverability of hybrid colloidal gels

Rheological studies were performed on different colloidal gels. A strong dependence of viscosity on different NP mass ratios (Fig. 5A) and NP concentrations (Fig. 5B) was observed. At the same NP concentration (20%), pure HAp NPs yielded the highest viscosity gel, presumably due to the tight structure and minimal porosity (Fig. 5A). Pure HAp NPs showed limited reversibility, however, during the forward-and-backward stress sweep experiments. This confirmed the poor cohesiveness of calcium phosphate ceramic paste, which may point to a substantial limitation of this material as a tissue engineering scaffold.

As expected, the addition of PLGA NPs to HAp NPs significantly improved cohesiveness of this material as evidenced by retention of viscosity after shear (Fig. 5A). Compared to other ratios, gels with more negatively charged NPs

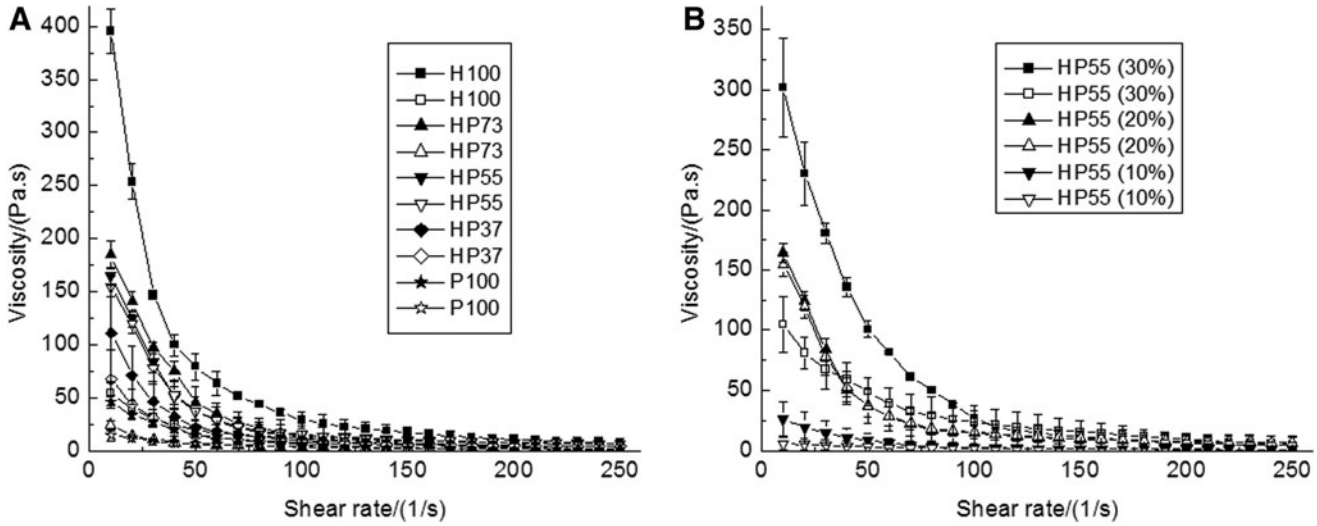

FIG. 5. Viscosity and shear thinning behavior of colloidal gels (20% concentration) mixed at different NP mass ratios **(A)** and HP55 colloidal gel at different concentrations **(B)** for accelerating (solid symbols) and decelerating (open symbols) the shear rate.

(HP73, 7:3 mass ratio of HAp to PLGA NPs, 20% concentration) yielded higher viscosity. On the contrary, gels with excess positive charged NPs (HP37, 3:7 mass ratio of HAp to PLGA NPs, 20% concentration) showed more fluidity. The 5:5 mass ratio recovered the original viscosity that was observed before shearing the material. The balance of positively charged and negatively charged NPs yielded a highly cohesive network that recovered quickly. Pure PLGA NP gels showed minimal shear thinning behavior (P100).

As the concentration of NPs was increased, higher viscosity and more shear thinning behavior were observed in the colloidal system (Fig. 5B). The HP55 colloidal gel at 20% concentration showed excellent recovery of the initial material viscosity. At 30% concentration, this same ratio yielded colloidal gels that did not recover viscosity to the same extent. This dynamic property may hinge upon a fine balance between particle concentration as well as the mass ratio of oppositely charged particles. For example, particle mobility may be hindered at higher concentrations, thus impeding restoration of interparticle interactions and slowing material recovery.

As colloidal systems, the cohesive strength depends upon interparticle interactions.[5] These electrostatic forces and van der Waals attractions were determined by the NP concentration and mass ratios of oppositely charged particles within the colloidal systems. Negatively charged HAp and positively charged PLGA NPs self-assembled through interparticle interactions to form a stable 3D porous structure. In static status, colloidal assemblies with a stable structure exhibit high viscosity at equilibrium (Fig. 4). Once the static status is disrupted, the gel system will exhibit pseudoplastic properties. If the external force is removed, the cohesion of the colloidal gel will be recovered and the 3D porous structure will be reconstructed. This unique recoverability makes the colloidal gel an excellent injectable material for applications in tissue engineering. All the results suggested that the hybrid HAp/PLGA NP colloidal gels were excellent injectable materials for bone regeneration applications, such as filling of irregular bone defects.

Negligible cytotoxicity of hybrid colloidal gels to hUCMSCs

Stem cells have the great potential to revolutionize traditional medicine with the ability to repair the diseased or damaged tissues. Preformed tissue scaffolds have many drawbacks, including in some cases, poor biocompatibility to the cells, difficulties in seeding cells, and complications with cell/material placement or retention during minimally invasive surgeries.[37,38] HAp/PLGA NP colloidal gels were tested to determine cell viability, since the viscoelastic properties of these materials are conducive to placement via injection.

hUCMSCs were isolated and cultured on HP73, HP55, or HP37 gels for up to 2 weeks. Cells treated without colloidal gels on blank polystyrene tissue culture plates were used as a control. Afterward, LIVE/DEAD viability assays were conducted to the scaffolds with cells. In these experiments, negligible cell death was observed in cell-loaded hybrid colloidal gels for 48 h and for 2 weeks (Fig. 6). This qualitative result demonstrated that hybrid HAp/PLGA NP colloidal gels possessed negligible cytotoxicity to hUCMSCs. Hence, resulted colloidal gels are potentially safe scaffolds for seeding stem cells. The high porosity and elasticity of the colloidal gels may contribute to this application.

Conclusions

In this article, a new colloidal gel system composed of negatively charged inorganic HAp NPs and positively charged organic PLGA NPs was demonstrated. The cohesive

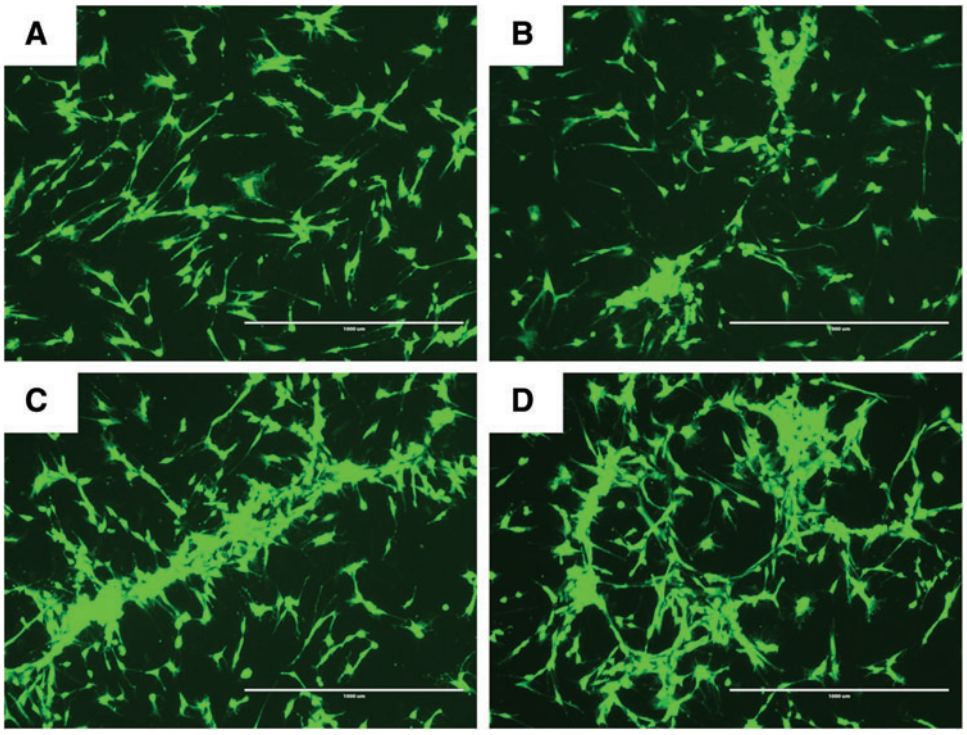

FIG. 6. Human umbilical cord mesenchymal stem cells cultured on colloidal gels HP 73 **(B)**, HP55 **(C)**, and HP37 **(D)** demonstrated high viability comparing to reference **(A)** treated without colloidal gels (scale bars were 1 mm). Color images available online at www.liebertpub.com/tea

strength of the gels derived from the interparticle interactions, such as electrostatic forces and van der Waals attraction. The unique response to external shear force and recoverable properties make this colloidal gel system an excellent candidate for injectable bone filling. Cytotoxicity tests also demonstrated negligible toxicity to hUCMSCs. In future research, stability tests will be carried out to investigate the effects of pH and ionic strength on the gels' properties. The integration of drug release strategies (e.g., small molecules and growth factors) will further explore for advanced applications for bone tissue engineering combined with local controlled drug release.

Acknowledgments

We gratefully acknowledge the Microscopy Laboratory for assistance with imaging. We are grateful for the support from funding agencies, such as the NIH (R01 DE022472) and the State of Kansas. We also extend our gratitude to the nursing staff for the assistance with umbilical cord harvesting at the Lawrence Memorial Hospital, Lawrence, Kansas.

Disclosure Statement

No competing financial interests exist.

References

1. Yelin, E.H., and Felts, W.R. A summary of the impact of musculoskeletal conditions in the United States. Arthritis Rheum **33,** 750, 2005.
2. Yelin, E., and Callahan, L.F. Special article the economic cost and social and psychological impact of musculoskeletal conditions. Arthritis Rheum **38,** 1351, 2005.
3. Kretlow, J.D., Young, S., Klouda, L., Wong, M., and Mikos, A.G. Injectable biomaterials for regenerating complex craniofacial tissues. Adv Mater **21,** 3368, 2009.
4. Hou, Q., Paul, A., and Shakesheff, K.M. Injectable scaffolds for tissue regeneration. J Mater Chem **14,** 1915, 2004.
5. Griffith, L.G., and Naughton, G. Tissue engineering—current challenges and expanding opportunities. Science **295,** 1009, 2002.
6. Li, Y.Y., Cunin, F., Link, J.R., Gao, T., Betts, R.E., Reiver, S.H., Chin, V., Bhatia, S.N., and Sailor, M.J. Polymer replicas of photonic porous silicon for sensing and drug delivery applications. Science **299,** 2045, 2003.
7. Wang, Q., Jamal, S., Detamore, M.S., and Berkland, C. PLGA-chitosan/PLGA-alginate nanoparticle blends as biodegradable colloidal gels for seeding human umbilical cord mesenchymal stem cells. J Biomed Mater Res A **96,** 520, 2011.
8. Gilchrist, J.F., Chan, A.T., Weeks, E.R., and Lewis, J.A. Phase behavior and 3D structure of strongly attractive microsphere-nanoparticle mixtures. Langmuir **21,** 11040, 2005.
9. Tohver, V., Chan, A., Sakurada, O., and Lewis, J.A. Nanoparticle engineering of complex fluid behavior. Langmuir **17,** 8414, 2001.
10. Johnson, S.A., Ollivier, P.J., and Mallouk, T.E. Ordered mesoporous polymers of tunable pore size from colloidal silica templates. Science **283,** 963, 1999.
11. Holtz, J.H., and Asher, S.A. Polymerized colloidal crystal hydrogel films as intelligent chemical sensing materials. Nature **389,** 829, 1997.
12. Chrisey, D.B. The power of direct writing. Science **289,** 879, 2000.
13. Klajn, R., Bishop, K.J.M., Fialkowski, M., Paszewski, M., Campbell, C.J., Gray, T.P., and Grzybowski, B.A. Plastic and moldable metals by self-assembly of sticky nanoparticle aggregates. Science **316,** 261, 2007.
14. Therriault, D., White, S.R., and Lewis, J.A. Chaotic mixing in three-dimensional microvascular networks fabricated by direct-write assembly. Nat Mater **2,** 265, 2003.
15. Wang, Q., Wang, L., Detamore, M.S., and Berkland, C. Biodegradable colloidal gels as moldable tissue engineering scaffolds. Adv Mater **20,** 236, 2008.
16. Wang, Q., Wang, J., Lu, Q., Detamore, M.S., and Berkland, C. Injectable PLGA based colloidal gels for zero-order dexamethasone release in cranial defects. Biomaterials **31,** 4980, 2010.
17. Büyüktimkin, B., Wang, Q., Kiptoo, P., Stewart, J.M., Berkland, C., and Siahaan, T.J. Vaccine-like controlled-release delivery of an immunomodulating peptide to treat experimental autoimmune encephalomyelitis. Mol Pharm **9,** 979, 2012.
18. Xie, B., Parkhill, R.L., Warren, W.L., and Smay, J.E. Direct writing of three-dimensional polymer scaffolds using colloidal gels. Adv Funct Mater **16,** 1685, 2006.
19. Dellinger, J.G., Cesarano III, J., and Jamison, R.D. Robotic deposition of model hydroxyapatite scaffolds with multiple architectures and multiscale porosity for bone tissue engineering. J Biomed Mater Res A **82,** 383, 2007.
20. Ginebra, M., Fernandez, E., De Maeyer, E., Verbeeck, R., Boltong, M., Ginebra, J., Driessens, F., and Planell, J. Setting reaction and hardening of an apatitic calcium phosphate cement. J Dent Res **76,** 905, 1997.
21. Zhao, L., Burguera, E.F., Xu, H.H.K., Amin, N., Ryou, H., and Arola, D.D. Fatigue and human umbilical cord stem cell seeding characteristics of calcium phosphate–chitosan–biodegradable fiber scaffolds. Biomaterials **31,** 840, 2010.
22. Zhao, L., Weir, M.D., and Xu, H.H.K. Human umbilical cord stem cell encapsulation in calcium phosphate scaffolds for bone engineering. Biomaterials **31,** 3848, 2010.
23. Ducheyne, P., and Qiu, Q. Bioactive ceramics: the effect of surface reactivity on bone formation and bone cell function. Biomaterials **20,** 2287, 1999.
24. Pilliar, R., Filiaggi, M., Wells, J., Grynpas, M., and Kandel, R. Porous calcium polyphosphate scaffolds for bone substitute applications—in vitro characterization. Biomaterials **22,** 963, 2001.
25. Deville, S., Saiz, E., Nalla, R.K., and Tomsia, A.P. Freezing as a path to build complex composites. Science **311,** 515, 2006.
26. Reilly, G.C., Radin, S., Chen, A.T., and Ducheyne, P. Differential alkaline phosphatase responses of rat and human bone marrow derived mesenchymal stem cells to 45S5 bioactive glass. Biomaterials **28,** 4091, 2007.
27. Can, A., and Karahuseyinoglu, S. Concise review: human umbilical cord stroma with regard to the source of fetus-derived stem cells. Stem Cells **25,** 2886, 2007.
28. Baksh, D., Yao, R., and Tuan, R.S. Comparison of proliferative and multilineage differentiation potential of human mesenchymal stem cells derived from umbilical cord and bone marrow. Stem Cells **25,** 1384, 2007.
29. Wang, H.S., Hung, S.C., Peng, S.T., Huang, C.C., Wei, H.M., Guo, Y.J., Fu, Y.S., Lai, M.C., and Chen, C.C. Mesenchymal stem cells in the Wharton's jelly of the human umbilical cord. Stem Cells **22,** 1330, 2004.
30. Karahuseyinoglu, S., Kocaefe, C., Balci, D., Erdemli, E., and Can, A. Functional structure of adipocytes differentiated

from human umbilical cord stroma-derived stem cells. Stem Cells **26,** 682, 2008.
31. Wang, L., Singh, M., Bonewald, L.F., and Detamore, M.S. Signalling strategies for osteogenic differentiation of human umbilical cord mesenchymal stromal cells for 3D bone tissue engineering. J Tissue Eng Regen Med **3,** 398, 2009.
32. Wang, Q., Zhang, N., Hu, X., Yang, J., and Du, Y. Chitosan/starch fibers and their properties for drug controlled release. Eur J Pharm Biopharm **66,** 398, 2007.
33. Wang, Q., Zhang, N., Hu, X., Yang, J., and Du, Y. Chitosan/polyethylene glycol blend fibers and their properties for drug controlled release. J Biomed Mater Res A **85,** 881, 2008.
34. Wang, Q., Du, Y., Fan, L., Liu, H., and Wang, X. Structures and properties of chitosan-starch-sodium benzoate blend films. Wuhan Univ J (Nat Sci Ed) **6,** 013, 2003.
35. Williams, S.J., Wang, Q., MacGregor, R.R., Siahaan, T.J., Stehno-Bittel, L., and Berkland, C. Adhesion of pancreatic beta cells to biopolymer films. Biopolymers **91,** 676, 2009.
36. Weiss, M.L., Medicetty, S., Bledsoe, A.R., Rachakatla, R.S., Choi, M., Merchav, S., Luo, Y., Rao, M.S., Velagaleti, G., and Troyer, D. Human umbilical cord matrix stem cells: preliminary characterization and effect of transplantation in a rodent model of Parkinson's disease. Stem Cells **24,** 781, 2005.
37. Laurencin, C.T., Ambrosio, A., Borden, M., and Cooper, J., Jr. Tissue engineering: orthopedic applications. Annu Rev Biomed Eng **1,** 19, 1999.
38. Hutmacher, D.W. Scaffolds in tissue engineering bone and cartilage. Biomaterials **21,** 2529, 2000.

Address correspondence to:
Qun Wang, PhD
Department of Chemical and Biological Engineering
Iowa State University
352 Town Engineering Building
Ames, IA 50011

E-mail: qunwang@iastate.edu

Cory Berkland, PhD
Department of Pharmaceutical Chemistry
University of Kansas
Multidisciplinary Research Building
2030 Becker Drive
Lawrence, KS 66047

E-mail: berkland@ku.edu

Received: January 31, 2013
Accepted: June 20, 2013
Online Publication Date: August 12, 2013